Cyclic Properties of $Li[Co_{0.17}Li_{0.28}Mn_{0.55}]O_2$ Cathode Material

Yong Joon Park,* Young-Sik Hong, Xianglan Wu, Min Gyu Kim,† Kwang Sun Ryu, and Soon Ho Chang

Power Source Device Team, Electronics and Telecommunications Research Institute, Daejeon 305-350, Korea
†Beamline Research Division, Pohang Accelerator Laboratory, Pohang University of Science and Technology, Pohang 790-784, Korea
Received May 20, 2003

A $Li[Co_{0.17}Li_{0.28}Mn_{0.55}]O_2$ cathode compound was prepared by a simple combustion method. The X-ray diffraction pattern showed that this compound could be classified as α-$NaFeO_2$ structure type with the lattice constants of a = 2.8405(9) Å and c = 14.228(4) Å. According to XANES analysis, the oxidation state of Mn and Co ions in the compound were 4+ and 3+, respectively. During the first charge process, the irreversible voltage plateau at around 4.65 V was observed. The similar voltage-plateau was observed in the initial charge profile of other solid solution series between Li_2MnO_3 and $LiMnO_2$ (M=Ni, Cr…). The first discharge capacity was 187 mAh/g and the second discharge capacity increased to 204 mAh/g. As the increase of cycling number, one smooth discharge profile was converted to two distinct sub-plateaus and the discharge capacity was slowly decreased. From the Co and Mn K-edge XANES spectra measured at different cyclic process, it can be concluded that irreversible transformation of phase is occurred during continuous cycling process.

Key Words : Cathode, Layered structure, Lithium battery, XANES, Cyclic properties

Introduction

Lithium cobalt oxide ($LiCoO_2$) is an useful cathode material with good electrochemical performances for lithium secondary battery. However, the relatively high cost of the cobalt and the lure of larger specific capacity have led to the study of other possible cathode materials. Recently, some groups investigated solid solution series between Li_2MnO_3 (or $Li[Li_{1/3}Mn_{2/3}]O_2$) and $LiMO_2$ (M=Cr, Ni, Co) as an alternative cathode material for $LiCoO_2$.[1-6] $Li[Li_{1/3}Mn_{2/3}]O_2$ is well-known to an electrochemically inactive material because the Mn^{4-} in $Li[Li_{1/3}Mn_{2/3}]O_2$ normally cannot be oxidized beyond the 4+ oxidation state in order to extract Li from its lattice. However, it is interesting that the solid solution series between $Li[Li_{1/3}Mn_{2/3}]O_2$ and $LiMO_2$ (M=Cr, Ni, Co) showed very high discharge capacity over 200 mAh/g when they cycled with an upper cut-off voltage of about 4.8 V.

Paulsen *et al.* reported that $Li[Li_{0.2}Cr_{0.4}Mn_{0.4}]O_2$ can be regarded as a solid solution between $Li[Li_{1/3}Mn_{2/3}]O_2$ and $LiCrO_2$.[7] Lu *et al.* also investigated solid solution series between $Li[Li_{1/3}Mn_{2/3}]O_2$ and $LiMO_2$ (M=Cr, Ni).[1-5] $Li[Ni_xLi_{(1/3-2x/3)}Mn_{(2/3-x/3)}]O_2$ and $Li[Cr_xLi_{(1/3-x/3)}Mn_{(2/3-2x/3)}]O_2$ were derived from $Li[Li_{1/3}Mn_{2/3}]O_2$ by substitution of Li^+ and Mn^{+4} by Ni^{2-} or Cr^{3+}, respectively. When the cells containing such oxides charged to about 4.8 V, it exhibited an irreversible capacity at around 4.5-4.7 V. After the first charge process, the cells were reversibly cycled with a high capacity of over 200 mAh/g in the voltage range of 2.0 and 4.8 V.

In the previous report,[8] we investigated the electrochemical properties of $Li[Ni_xLi_{(1/3-2x/3)}Mn_{(2/3-x/3)}]O_2$ compounds prepared by the simple combustion method. Compared to mixed hydroxide or sol-gel methods adopted by other researcher, the simple combustion method is very simple and it will cut down the manufacturing cost of cathode powders. Among the various compositions in the previous work,[8] the $Li[Ni_{0.17}Li_{0.22}Mn_{0.61}]O_2$ compound (x = 0.17 in $Li[Ni_xLi_{(1/3-2x/3)}Mn_{(2/3-x/3)}]O_2$) showed the largest specific capacity and the most stable cycle performance.

In this study, $Li[Co_{0.17}Li_{0.28}Mn_{0.55}]O_2$ cathode material, which composition is x=0.17 in $Li[Co_xLi_{(1/3-x/3)}Mn_{(2/3-2x/3)}]O_2$, was prepared by the simple combustion method. The stoichiometry of $Li[Co_xLi_{(1/3-x/3)}Mn_{(2/3-2x/3)}]O_2$ is determined from the assumption that transition metal Co and Mn are in the oxidation states of +3 and +4, respectively. This compound can be derived from $Li[Li_{1/3}Mn_{2/3}]O_2$ by substitution of Li^- and Mn^{-4} by Co^{3+} and also classified solid solution series between $LiCoO_2$ (17%) and $Li[Li_{1/3}Mn_{2/3}]O_2$ (83%). The structure and electrochemical properties of the powder were investigated using XRD and charge/discharge method. Specially, phase transformation during the cycling was observed by XANES analysis.

Experimental Section

$Li[Co_{0.17}Li_{0.28}Mn_{0.55}]O_2$ was prepared by the simple combustion method from manganese acetate tetrahydrate [$Mn(CH_3CO_2)_2{\cdot}4H_2O$], cobalt(III) nitrate hexahydrate [$Co(NO_3)_2{\cdot}6H_2O$], lithium acetate dihydrate [$CH_3CO_2Li{\cdot}2H_2O$] and lithium nitrate [$LiNO_3$]. At first, a stoichiometric amount of source materials of Co, Ni and Li were mixed with distilled water and continuously stirred at 100 °C on a hot plate. After evaporation of excess water, a viscous gel with green color was obtained. When the resulting gel was fired around 400 °C, a vigorous decomposition process of organic material occurred accompanying ash like powders.

*Corresponding Author: Tel: +82-42-860-5516; Fax: +82-42-860-6836; e-mail: yjpark@etri.re.k

The decomposed powder was ground and heated at 500 °C for 3 hours. The heat-treated powder was re-ground and re-heated at 1000 °C in air for 6 hours. Then, it was cooled down to room temperature within a few minutes.

X-ray diffraction (XRD) data were collected using Philips X-ray diffractometer in the 2θ range from 15 to 70° with Cu-K_α radiation (λ = 1.5406 Å). The electrochemical cell was assembled in a dry room using the $Li[Co_{0.17}Li_{0.28}Mn_{0.55}]O_2$ powder, lithium, porous polyethylene film and 1 M $LiPF_6$ solution in 1 : 1 volume ratio of ethylene carbonate/dimethyl carbonate. For the preparation of positive electrode, 0.4 g of polyvinyl difluoride (Aldrich) was dissolved in about 25 g N-methyl-2-pyrrolidone for one hour and then 4 g of $Li[Co_{0.17}Li_{0.28}Mn_{0.55}]O_2$ powder and 0.6 g of Super P black (MMM Carbon Co.) were added. After a day of ball mill process, viscous slurry was coated on an aluminum foil using a doctor blade and obtained a film with uniform thickness. After then, it was dried at 90 °C in an oven. The obtained cathode film was hot pressed at 135 °C to increase tap density. The thickness of the cathode film was about 30 μm. Cyclic voltammograms were measured from the test cells by a Biologic Mac Pile II potentiostat. Sweep range and scan rate were 2.0-5.0 V and 0.05 mVS^{-1}, respectively. The galvanostatic charge-discharge test was carried out using Toyo charge-discharge system. The test cells were charged up to 4.8 or 4.6 V versus Li/Li^+ with a specific current of 20 mA/g, and then discharged to 2.0 V with the same specific current.

The XANES (X-ray absorption near-edge structure) measurement was carried out during initial charge-discharge process. In detail, cathodes separated from the cell were washed with dimethyl carbonate (DMC) solution and dried in a vacuum oven. These cathodes were put into Mylar film bag and sealed in a glove box to prevent contamination. The Co and Mn K-edge X-ray absorption spectra recorded on the BL7C1(EC) beam line of Pohang Light Source (PLS) with the ring current of 140-170 mA at 2.5 GeV. Si(311) double crystal monochromator has been used with detuning to 75% in intensity to eliminate high-order harmonics. The data have been collected in transmission mode with the nitrogen gas-filled ionization chambers as detectors. In order to remove an energy shift problem, X-ray absorption spectra for the metal foils has been measured simultaneously in every measurement as the metal foil was positioned in front of the window of the third ion chamber.

Results and Discussion

Figure 1 shows the X-ray diffraction patterns of $Li[Co_{0.17}Li_{0.28}Mn_{0.55}]O_2$ compound and references materials. Small XRD peaks between 20 and 25° are attributed to the superlattice ordering of Li and Mn in the transition-metal containing layers.[3-6] Except for the superlattice peaks, all peaks of the XRD patterns can be indexed to α-$NaFeO_2$ structure (space group: $R\bar{3}m$) with lattice constant of a = 2.8405(9) Å and c = 14.228(4) Å. A c/a ratio is 5.009, indicating a layer structure. In the previous reports,[9,10]

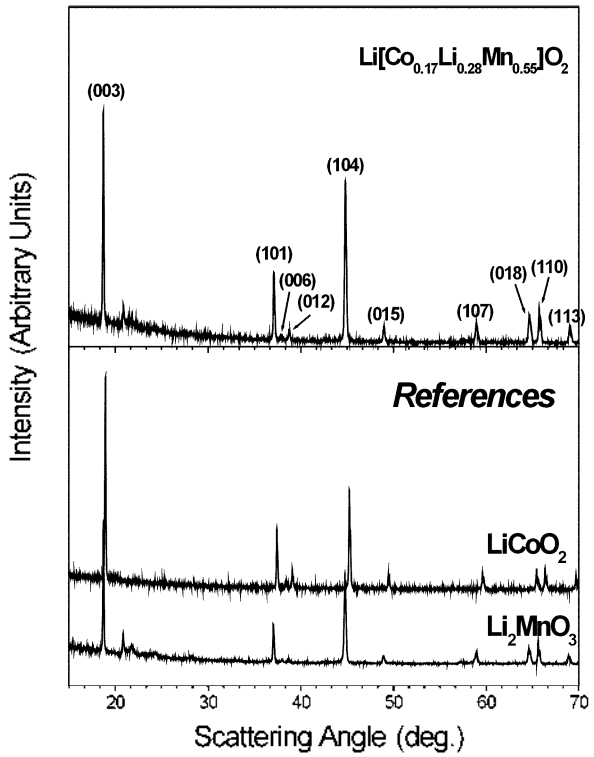

Figure 1. X-ray diffraction patterns of $Li[Co_{0.17}Li_{0.28}Mn_{0.55}]O_2$ compound and references.

similar compound was prepared by a calcination of the source-mixture with constituent elements. However, this method did not successfully form a single phase without excess Li_2O. By contrast, the simple combustion method used in this work makes possible to form a single phase without excess Li_2O.

To examine a oxidation state of Mn and Co, the K-edge XANES spectra for fresh $Li[Co_{0.17}Li_{0.28}Mn_{0.55}]O_2$ compound were measured. The K-edge XANES spectra of Li_2MnO_3 and $LiCoO_2$ were used as references because Mn oxidation state in Li_2MnO_3 and Co oxidation state in $LiCoO_2$ are already known to 4− and 3−, respectively. Figure 2a shows the Mn K-edge XANES spectra for $Li[Co_{0.17}Li_{0.28}Mn_{0.55}]O_2$ and Li_2MnO_3. The edge position and spectrum-shape of $Li[Co_{0.17}Li_{0.28}Mn_{0.55}]O_2$ compound are the same as those of Li_2MnO_3, which indicates that Mn oxidation state in $Li[Co_{0.17}Li_{0.28}Mn_{0.55}]O_2$ compound is 4−. The very similar edge positions of Co K-edge XANES spectra between $Li[Co_{0.17}Li_{0.28}Mn_{0.55}]O_2$ and $LiCoO_2$ are displayed in Figure 2b. This shows Co oxidation state in $Li[Co_{0.17}Li_{0.28}Mn_{0.55}]O_2$ compound is same as that in $LiCoO_2$ (Co^{3+}). But, a slight difference of spectra-shape implies that there may be a little difference of Co-Co long-range patterns between two compounds.[11] According to the XRD and XANES analyses, it is clear that the $Li[Co_{0.17}Li_{0.28}Mn_{0.55}]O_2$ compound prepared in this work shows a single phase compound with Mn^{4-} and Co^{3-} oxidation states.

The electrochemical property of the compound is investigated from a test cell. Figure 3 shows the cyclic voltammogram for the compound at a sweep range of 2.0-5.0 V with

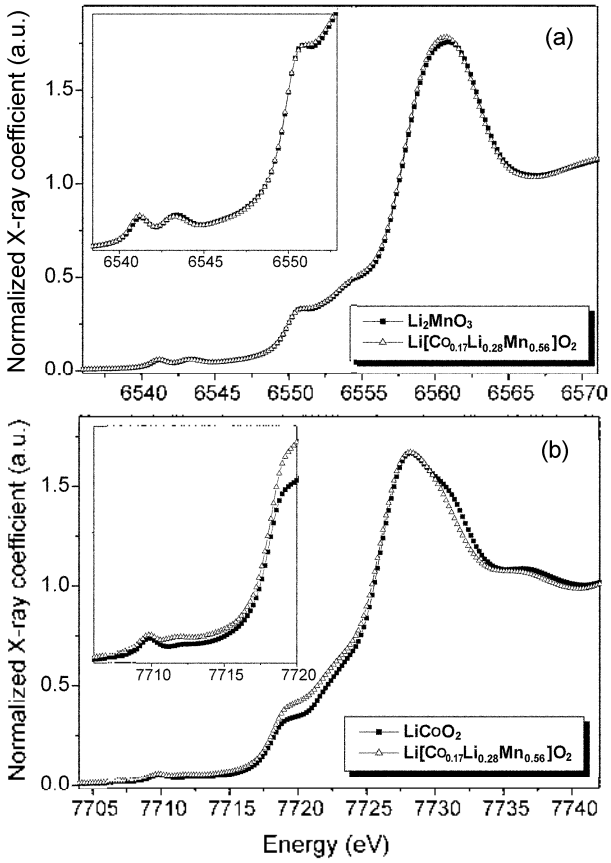

Figure 2. (a) Mn K-edge XANES spectra for $Li[Co_{0.17}Li_{0.28}Mn_{0.55}]O_2$ compound and Li_2MnO_3; (b) Co K-edge XANES spectra for $Li[Co_{0.17}Li_{0.28}Mn_{0.55}]O_2$ compound and $LiCoO_2$.

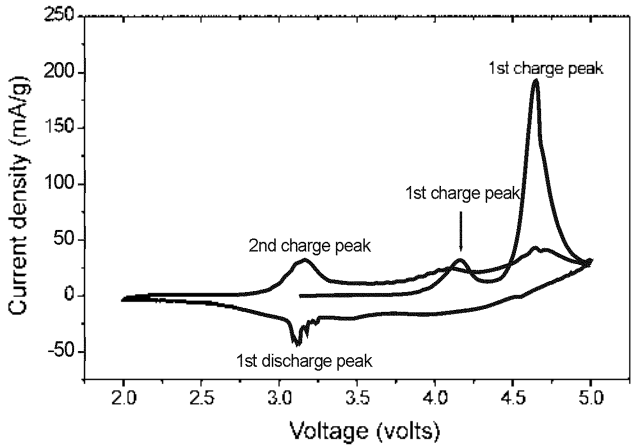

Figure 3. Cyclic voltammogram for $Li[Co_{0.17}Li_{0.28}Mn_{0.55}]O_2$ compound. The peaks detected during 1st and 2nd cycling are marked. Scan rate = 0.05 mVS^{-1}.

scan rate of 0.05 mVS^{-1}. Two peaks at around 4.15 and 4.65 V appear in the initial oxidation step. Specially, a large peak at 4.65 V means that there is a long voltage plateau at around this range during first charge process. By contrast, only one peak at around 3.15 V is observed in the subsequent reduction and oxidation curves. This suggests that the irreversible phase transition is occurred during the initial charge process.

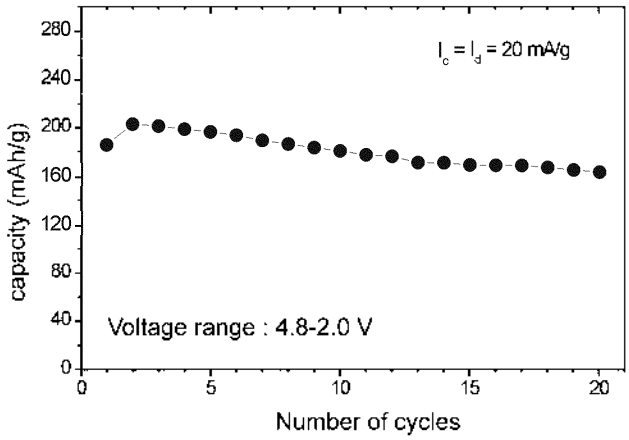

Figure 4. Cyclic performances for $Li[Co_{0.17}Li_{0.28}Mn_{0.55}]O_2$ compound between 4.8 and 2.0 V at a constant specific current of 20 mA/g.

Similar irreversible phase transformation has been investigated in the solid-solution series between $Li[Li_{1/3}Mn_{2/3}]O_2$ and $LiMO_2$ (M=Cr, Ni, Co).[1-6] Lu *et al.* suggested that the irreversible plateau occurred due to the simultaneous extraction of both Li and O from the material.[1-5] They assumed that the portion of the first charge to 4.45 V correspond to deintercalation of lithium and oxidation of metal ion (Cr, Ni) and the plateau at about 4.5-4.7 V correspond to the removal of the remaining lithium from the lithium layer, along with the simultaneous ejection of oxygen. On the contrary, Robertson and Bruce have presented that the exchange of Li^+ by H^+ in non-aqueous media results in the long irreversible plateau.[12,13] The origin of the plateau and phase transformation during first charge process is still remained unsolved.

Figure 4 shows the discharge capacity vs. the cycle number of a test cell using the $Li[Co_{0.17}Li_{0.28}Mn_{0.55}]O_2$ compound. The specific current and voltage range were 20 mA/g and 4.8-2.0 V, respectively. The compound delivers the 1st discharge capacity of 187 mAh/g. The 2nd discharge capacity increased to 204 mAh/g, however, after the 2nd cycle, the capacity slowly decreased as the increase of cycle number. The 1st, 5th, 10th and 20th charge-discharge curves in the voltage range of 2.0-4.8 V are shown in Figure 5a. After the 1st charge curve with long voltage plateau, the 1st discharge curve shows smooth profile. This smooth charge-discharge curve after initial charge process corresponds to other solid-solution series between $Li[Li_{1/3}Mn_{2/3}]O_2$ and $LiMO_2$ (M=Cr, Ni). However, as the increase of cycle number, smooth profile is slowly converted to two sub-plateaus, which indicates that the structure of $Li[Co_{0.17}Li_{0.28}Mn_{0.55}]O_2$ compound is transformed to a spinel phase. This finding is unexpected result since other solid solution series between $Li[Li_{1/3}Mn_{2/3}]O_2$ and $LiMO_2$ (M=Cr, Ni) are stable after initial charge process. To investigate the effect of voltage range, the cut-off voltage during the charge process is lowered from 4.8 to 4.6 V. Figure 5b shows the change of voltage profile measured in the voltage range of 2.0-4.6 V. The sub-plateau in the discharge profile measured at 20th cycle becomes a

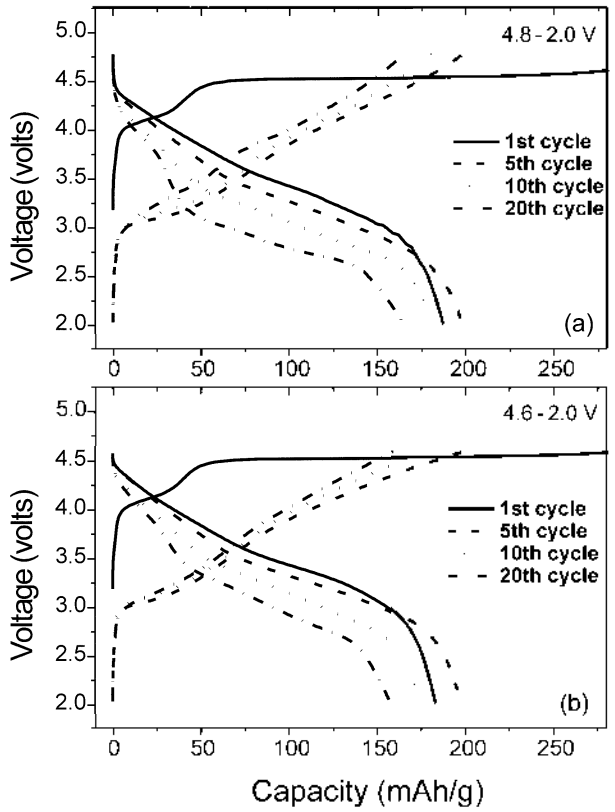

Figure 5. 1st, 5th, 10th and 20th voltage profile of $Li[Co_{0.17}Li_{0.28}Mn_{0.55}]O_2$ compound in the voltage range of (a) 4.8-2.0 V; (b) 4.6-2.0 V at a constant specific current of 20 mA/g.

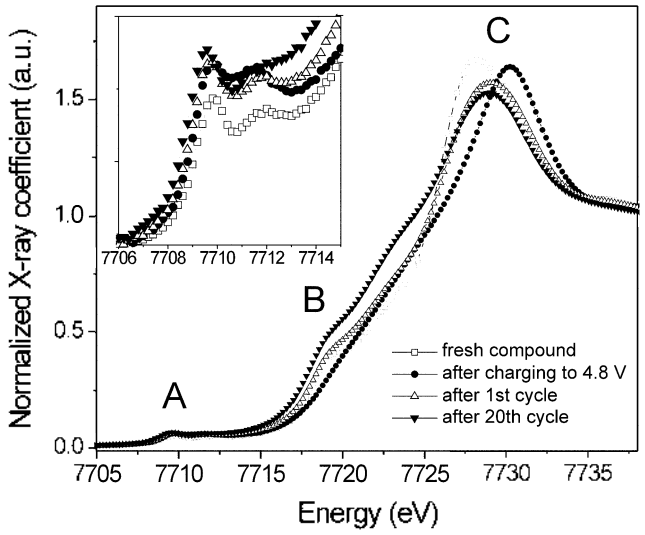

Figure 6. Co K-edge XANES spectra for $Li[Co_{0.17}Li_{0.28}Mn_{0.55}]O_2$ compound measured at different cyclic process.

slight faint, but phase transformation is still observed.

X-ray absorption near-edge structure (XANES) analysis is performed to get more information about change of electronic structure during cycling process. Figure 6 shows the Co K-edge XANES spectra for the compound measured at different cyclic process. For the fresh compound, a weak absorption peak A at 7709.6 eV represents the transition of 1s electron to an unoccupied 3d-e_g orbital of Co^{3-} ion with low spin (t_{2g}^6) electronic configuration.[11] Although the 1s → 3d transition is electric dipole-forbidden transition in an ideal octahedral symmetry, the appearance of weak absorption peak is due to pure electric quadrupole coupling and noncentrosymmetric environment of slightly distorted CoO_6 octahedral site.[11] Both peaks B and C appear from the electric dipole-allowed transition of a 1s core electron to an unoccupied 4p bound state with T_{1u} symmetry. The peaks B and C correspond to two final states of a $1s^1\underline{c}3d^7\underline{L}4p^1$ with shakedown process by ligand to metal charge transfer (LMCT) and a $1s^1\underline{c}3d^64p^1$ without shakedown process, respectively, where $\underline{c}$ and $\underline{L}$ indicate a 1s core hole and a ligand hole. The shoulder peak B occurs on the lower energy region of about 10 eV with respect to main absorption C peak at 7729 eV since the 1s core electron of $3d^7\underline{L}$ state is less bounded on the more screened nucleus with respect to that of $3d^6$ state.

When the $Li[Co_{0.17}Li_{0.28}Mn_{0.55}]O_2$ compound charged to 4.8 V, the edge position of the Co K-edge XANES spectrum shifts to higher energy value. This positive shift shows the increase of average oxidation state of Co ion from 3− to about 4−. The significant decrease of peak B at the charging to 4.8 V means that the delithiation gives rise to transition of hole state ($\underline{L}$) from oxygen to Co atom. On the delithiation, the $|3d^7\underline{L}>$ state of LMCT process is replaced by the $|3d^5>$ state of Co^{4+} ion as an another hole state, which means that the hole state is relatively localized at Co atomic site under the local structural distorted environment. The abrupt disappearance of peak B can be also another hint about the local structural distortion by the formation of Co^{4-} ion, in addition to the increase of intensity of peak A.

The spectra marked 'after 1st cycle' and 'after 20th cycle' are measured from a sample discharged to 2.0 V after charging to 4.8 V. After 1st cycle, the edge position back to lower energy value, indicating the reduction of Co ion to lower oxidation state. However, the shape of Co K-edge spectra slightly changed from the pristine state, which corresponds to the irreversible phase transformation during the first cycle. After 20th cycle, more peak-shape change is observed in the Co K-edge spectrum for the compound. Specially, a weak shoulder peak is newly appeared at around ~7725 eV. This change may be attributed to the structural transformation during cycling.

The Mn K-edge XANES spectra for the compound measured at different cyclic process are shown in Figure 7. According to Figure 2, Mn oxidation state in fresh compound is 4+. In the pre-edge region A, spectra display a weak double-peak structure. It is assigned to 1s → 3d transition, which are observed with weak intensity for octahedral coordination and strong intensity for tetrahedral coordination ones.[12,13] The experimental spectra are consistent with octahedral or near-octahedral coordination of manganese. The intermediate bump at 6550 eV is very prominent for pristine sample. Its magnitude is related to the connectivity between MnO_6 octahedra in the structure.[14,15] After the sample was charged to 4.8 V, the shape of the near-edge spectrum in the region B

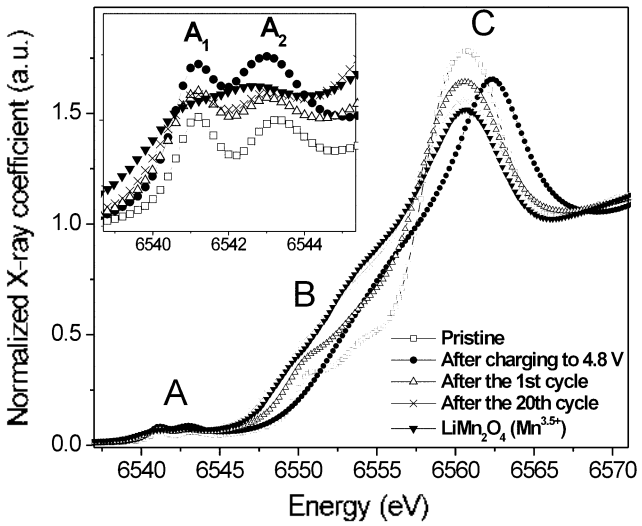

Figure 7. Mn K-edge XANES spectra for $Li[Co_{0.17}Li_{0.28}Mn_{0.55}]O_2$ compound measured at different cyclic process. The spectrum of $LiMn_2O_4$ ($Mn^{3.5+}$) is used as reference.

and C was significantly changed. This result does not present increase of Mn oxidation state because Mn^{4-} normally cannot be oxidized beyond 4+ in an octahedral oxygen environment.[16,17] This change can be explained by possible rearrangement of the Mn local structure.[18] The intermediate bump at 6550 eV also disappears because of the increase of local distortion around Mn site and the following decrease of overlap integral between Mn-O bondings.

The spectra marked after the 1st cycle and after the 20th cycle were measured from the discharged samples cycled between 2.0-4.8 V. The spectrum measured after the 1st cycle showed a slight negative shift compared with that of pristine state. It suggests that the Mn oxidation state is slightly decreased to less than 4+ although the local structure around Mn site is reversible with reappearance of the intermediate bump. But, the pre-edge peak intensity (peak A_2) in the higher energy region for 1st cycle is larger than that of $LiMn_2O_4$. Since the peak A_1 and A_2 correspond to electronic transition to unoccupied t_{2g} and e_g energy levels, respectively, the fact means the Mn^{4-} is relatively rich in the 1st cycle.

More shift of the edge position to negative direction was occurred after the 20th cycle. This Mn K-edge XANES spectrum is almost very similar with that of $LiMn_2O_4$ with coexistence of Mn^{3-} and Mn^{4+} ions. Therefore, it suggests that the Mn oxidation state in the compound decreased to about 3.5− after the 20th cycle. This result can be explained by the phase conversion from layered to spinel-like structure. According to the Shiraishi *et al.*, the region B and C can be ascribed mainly to the Mn^{3+} and Mn^{4-} in $LiMn_2O_4$ compound, respectively.[19] The intermediate bump is almost disappeared after 20 cycles, which suggests that the connectivity between MnO_6 octahedra in the structure is destroyed during cycling.

As mentioned earlier, this phase transformation during cycling is unexpected. Similar solid solutions of $Li[Ni_xLi_{(1/3-2x/3)}Mn_{(2/3-x/3)}]O_2$ is not detected decrease of Mn oxidation state after 20th cycle.[20] However, Robertson *et al.* reported that Li_2MnO_3 converted to spinel-like phase on cycling.[16,21] They suggested proton exchange between Li^+ in the oxide and H^- in the electrolyte is a main reason of electrochemical activity of Li_2MnO_3. This reaction is partially reversible, so the compound converts spinel-like phase during cycling.

In the case of $Li[Co_{0.17}Li_{0.28}Mn_{0.55}]O_2$ compound, which is a solid solution between Li_2MnO_3 and $LiCoO_2$, shows similar phase transition with Li_2MnO_3. The phase transformation can give negative effect to cycle performance of the compound. However, Armstrong *et al.* reported that the spinel-like material formed during intercalation processes from layered structure have better reversibility compared with the spinel phase prepared at high temperature.[22,23] Considering high discharge capacity and simple processing method, this material can be adopted as a possible cathode material if cycle life can be improved.

Conclusions

$Li[Co_{0.17}Li_{0.28}Mn_{0.55}]O_2$ compound was prepared by a simple combustion method. This method makes possible form a single phase without excess Li_2O. Except for the superlattice peaks, all peaks of the XRD patterns can be indexed to a-$NaFeO_2$ structure (space group: *R3m*) with the lattice constant of a = 2.8405(9) Å and c = 14.228(4) Å. From the comparison of XANES spectra with those of Li_2MnO_3 and $LiCoO_2$, the oxidation states of Mn and Co ion in the fresh compound were confirmed to 4+ and 3−, respectively. The irreversible voltage-plateau at 4.65 V is general result for solid-state series between Li_2MnO_3 and $LiMO_2$ (M=Ni, Co, Cr). The compound delivers a first discharge capacity of 187 mAh/g. Although the second discharge capacity increased to 204 mAh/g, due to the irreversible phase transformation, the capacity slowly decreased as the increase of cycle number.

Acknowledgement. This work was supported by the Korea Ministry of Information and Communication (MIC) (No. 2003-S-003).

References

1. Lu, Z.; MacNeil, D. D.; Dahn, J. R. *Electrochem. Solid-State Lett.* **2001**, *4*(11), A191.
2. Lu, Z.; Beaulieu, L. Y.; Donaberger, R. A.; Thomas, C. L.; Dahn, J. R. *J. Electrochem. Soc.* **2002**, *149*(6), A778.
3. Lu, Z.; Dahn, J. R. *J. Electrochem. Soc.* **2002**, *149*(11), A1454.
4. Lu, Z.; Dahn, J. R. *J. Electrochem. Soc.* **2002**, *149*(7), A815.
5. Lu, Z.; MacNeil, D. D.; Dahn, J. R. *Electrochem. Solid-State Lett.* **2001**, *4*(12), A200.
6. MacNeil, D. D.; Lu, Z.; Dahn, J. R. *J. Electrochem. Soc.* **2002**, *149*(10), A1332.
7. Paulsen, J. M.; Ammundsen, B.; Desilvestro, H.; Steiner, R.; Hassell, D. *The Electrochemical Society Meeting Abstracts*: Phoenix, AZ, Oct22-27, 2000; Vol 2000-2.
8. Park, Y. J.; Hong, Y.-S.; Wu, X.; Ryu, K. S.; Chang, S. H. *J. Power Sources* **2004**, accepted.
9. Numata, K.; Sakaki, C.; Yamanaka, S. *Chem. Lett.* **1997**, 725.

10. Numata, K.; Sakaki, C.; Yamanaka, S. *Solid State Ionics* **1999**, *117*, 257.
11. Kim, M. G.; Yo, C. H. *J. Phys. Chem. B* **1999**, *103*, 6457.
12. Manceau, A.; Corshkov, A. I.; Drits, V. A. *Am. Miner.* **1992**, *77*, 1133.
13. Hwang, S.-J.; Park, H.-S.; Choy, J.-H.; Campet, G. *J. Phys. Chem. B* **2001**, *105*, 335.
14. Ibarra-Palos, A.; Strobel, P.; Proux, O.; Hazemann, J. L.; Anne, M.; Morcrette, M. *Electrochim. Acta* **2002**, *47*, 3171.
15. Morcrette, M.; Barboux, P.; Perriere, J.; Brousse, T.; Traverse, A.; Boilot, J. P. *Solid State Ionics* **2001**, *138*, 213.
16. Robertson, A. D.; Bruce, P. G. *Chem. Mater.* **2003**, *15*, 1984.
17. Ammundsen, B.; Paulsen, J. *Adv. Mater.* **2001**, *13*, 943.
18. Balasubramanian, M.; McBreen, J.; Davidson, I. J.; Whitfield, P. S.; Kargina, I. *J. Electrochem. Soc.* **2002**, *149*, A176.
19. Shiraishi, Y.; Nakai, I.; Tsubata, T.; Himeda, T.; Nichikawa, F. *J. Solid State Chem.* **1997**, *133*, 587.
20. Park, Y. J.; Kim, M. G.; Hong, Y.-S.; Wu, X.; Ryu, K. S.; Chang, S. H. *Solid State Commun.* **2003**, *127*, 509.
21. Robertson, A. D.; Bruce, P. G. *Chem. Commun.* **2002**, 2790.
22. Armstrong, A. R.; Robertson, A. D.; Bruce, P. G. *Electrochemica Acta* **1999**, *45*, 285.
23. Armstrong, A. R.; Robertson, A. D.; Gitzendanner, R.; Bruce, P. G. *J. Solid State Chem.* **1999**, *145*, 549.